PRMT4 inhibitor TP-064 impacts both inflammatory and metabolic processes without changing the susceptibility for early atherosclerotic lesions in male apolipoprotein E knockout mice

Zhang, Y.; Verwilligen, R.A.F.; Boer, M. de; Sijsenaar, T.J.P.; Eck, M. van; Hoekstra, M.

Atherosclerosis 338 (2021) 23–29

Contents lists available at ScienceDirect

Atherosclerosis

journal homepage: www.elsevier.com/locate/atherosclerosis

PRMT4 inhibitor TP-064 impacts both inflammatory and metabolic processes without changing the susceptibility for early atherosclerotic lesions in male apolipoprotein E knockout mice

Yiheng Zhang *, Robin A.F. Verwilligen, Miriam de Boer, Timothy J.P. Sijsenaar, Miranda Van Eck, Menno Hoekstra

Division of BioTherapeutics, Leiden Academic Centre for Drug Research (LACDR), Leiden University, Gorlaeus Laboratories, Einsteinweg 55, 2333CC, Leiden, the Netherlands

ARTICLE INFO

Keywords:
Gene expression
CARM1
Atherosclerosis
Obesity
PPARgamma

ABSTRACT

Background and aims: Atherosclerotic cardiovascular disease is a metabolic and inflammatory disorder. *In vitro* studies have suggested that protein arginine methyltransferase 4 (PRMT4) may act as a transcriptional coactivator to modulate inflammatory and metabolic processes. Here we investigated the potential anti-atherogenic effect of PRMT4 inhibitor TP-064 *in vivo*.

Methods: Male apolipoprotein E knockout mice fed a high cholesterol/high fat Western-type diet were intraperitoneally injected three times a week with 2.5 mg/kg (low dose) or 10 mg/kg (high dose) TP-064 or with DMSO control.

Results: TP-064 induced a dose-dependent decrease in lipopolysaccharide-induced *ex vivo* blood monocyte Tnfα secretion ($p < 0.05$ for trend) in the context of unchanged blood monocyte concentrations and neutrophilia induction ($p < 0.01$ for trend). A dose-dependent decrease in gonadal white adipose tissue expression levels of PPARγ target genes was detected, which translated into a reduced body weight gain after high dose TP-064 treatment ($p < 0.05$). TP-064 treatment also dose-dependently downregulated gene expression of the glycogen metabolism related protein G6pc in the liver ($p < 0.001$ for trend). In addition, a trend towards lower plasma insulin and higher blood glucose levels was observed, which was paralleled by a reduction in hepatic mRNA expression levels of the insulin-responsive genes *Fasn* (−55%; $p < 0.001$) and *Gck* (−47%; $p < 0.001$) in high dose-treated mice. Plasma triglyceride levels were reduced by high dose TP-064 treatment (−30%; $p < 0.05$). However, no change was observed in the size or composition of aortic root atherosclerotic lesions.

Conclusions: The PRMT4 inhibitor TP-064 impacts both inflammatory and metabolic processes without changing atherosclerosis susceptibility of male apolipoprotein E knockout mice.

1. Introduction

Atherosclerosis, the primary underlying cause of cardiovascular disease, is a chronic inflammatory disease characterized by the accumulation of lipids and inflammatory monocyte-derived macrophages within the arterial wall [1]. Recent findings have identified the transcriptional activator protein arginine methyltransferase 4 (PRMT4), also known as coactivator-associated arginine methyltransferase 1 (CARM1), as a possible novel therapeutic target for combating atherosclerosis. PRMT4 belongs to the PRMT family of enzymes that methylate arginine residues to generate asymmetric dimethylarginine (ADMA) and symmetric dimethylarginine (SDMA) [2–4]. Through this methylating action, PRMTs can influence a variety of cellular activities, i.e., they regulate cell proliferation and modulate transcription by acting as coactivators/corepressors [5]. PRMT4 expression is upregulated in blood monocytes of atherosclerotic patients as compared to non-diseased subjects and positively correlated with gene expression levels of pro-inflammatory chemokines [6]. In further support to the hypothesis that PRMT4 is a potential promoter of inflammation in atherosclerosis, Covic et al. have shown that PRMT4 activity stimulates pro-inflammatory/pro-atherogenic cytokine protein expression in mouse fibroblasts [7]. In addition, we have shown that treatment with

* Corresponding author.
E-mail address: y.zhang.43@lacdr.leidenuniv.nl (Y. Zhang).

https://doi.org/10.1016/j.atherosclerosis.2021.11.001
Received 19 July 2021; Received in revised form 6 October 2021; Accepted 2 November 2021
Available online 8 November 2021

PRMT4 inhibitor TP-064 is able to block pro-inflammatory gene expression and cytokine secretion by macrophages *in vitro* and *ex vivo* [8].

In vitro, PRMT4 regulates a variety of cellular signaling pathways and biological activities [9–12]. For instance, Yadav et al. have suggested that PRMT4 is a crucial component in peroxisome proliferator-activated receptor gamma (PPARγ)-mediated adipocyte differentiation [13]. Kim et al. have also identified PRMT4 as a key regulator of high glucose-induced insulin secretion from pancreatic beta cells [14]. In addition, the total body glycogen metabolism can be regulated by PRMT4, since it controls the transcription of the glucose–6-phosphatase catalytic subunit (*G6pc*) in hepatocytes and glycogen synthase 1 (*Gys1*) and glycogen phosphorylase muscle associated (*Pygm*) in muscle cells[15][16].

Importantly, the physiological and pathological relevance of PRMT4 *in vivo* is still not fully understood. Embryos with a targeted disruption of PRMT4 are small in size and die perinatally due to lung anomalies, indicating the importance of PRMT4 for life but also compromising studies on the role of PRMT4 in other pathologies [17]. Recent studies have identified TP-064 and EZM2302 as selective and potent inhibitors of PRMT4 function [8,10,18,19]. In light of our previous findings that *in vivo* TP-064 treatment is effective in blocking PRMT4-related inflammatory activities [8], in the current study we applied TP-064 treatment in male hypercholesterolemic apolipoprotein E knockout ($apoe^{-/-}$) mice that are genetically susceptible to the development of atherosclerosis [20] to test the hypothesis that atherogenesis can be restricted by inhibiting PRMT4.

2. Materials and methods

2.1. Experimental animals

Male $apoe^{-/-}$ mice (10 weeks old, n = 10) were bred at the Gorlaeus Laboratories of the Leiden Academic Centre for Drug Research (LACDR) in Leiden, The Netherlands. Mice were housed in groups at a 12h light/dark cycle and had *ad libitum* access to food and water. During the experiments, the mice were fed a Western-type diet (WTD; Special Diet Services, Sussex UK) and were injected intraperitoneally three times a week with 10 μL of the PRMT4 inhibitor TP-064 or DMSO as solvent control. Previously, we have shown that at a dose of 10 mg/kg TP-064 treatment is effective in blocking PRMT4 mediated gene expression in the liver in mice [8]. However, since 10 mg/kg TP-064 treatment also induced (unwanted) neutrophilia [8], in the current study we included a 2.5 mg/kg TP-064 group to test the overall effectivity of this lower dosage and potentially show effect dose-dependency. After 3 weeks of treatment, one mouse in the 10 mg/kg treatment group was found dead in the cage without an obvious reason. As such, after 6 weeks of treatment, 10 mice in the control and low dose groups and 9 mice in the high dose group were sacrificed. Hereto, mice were anaesthetized at 2 h after the last TP-064 injection through subcutaneous administration of a mixture of 70 mg/kg xylazine, 1.8 mg/kg atropine, and 350 mg/kg ketamine. Under deep anesthesia, as monitored by the absence of the leg withdrawal reflex, mice were killed by exsanguination. Orbital blood was collected in EDTA-coated tubes (Greiner Bio One, Kremsmünster, Austria). The number of monocytes, lymphocytes and neutrophils in blood samples was measured using an automated Sysmex XT-2000iV Veterinary Hematology analyzer (Sysmex Corporation, Etten-Leur, The Netherlands). Subsequently, the diaphragm was severed, and the organs were perfused with PBS via the left ventricle of the heart. Organs were harvested and fixed in 3.7% formalin (Formal-fixx; Shandon Scientific Ltd, UK) for 24 h and stored in 0.1% sodium azide in PBS until histological analysis. The remaining organ parts were snap-frozen in liquid nitrogen and stored at −20 °C until further analysis.

All experimental protocols were approved by the Animal Welfare Body of Leiden University and were performed in compliance with the project license AVD1060020185964 issued by the Central Authority for Scientific Procedures on Animals (CCD) and were performed in accordance with the principles of laboratory animal care and regulations of Dutch law on animal welfare, the directive 2010/63/EU of the European Union, and the ARRIVE guidelines.

2.2. Enzyme-linked immunosorbent assay (ELISA)

The concentration of monocyte chemoattractant protein-1 (Mcp-1; BD Biosciences and Biolegend; San Jose and San Diego, CA, USA) and mouse serum amyloid P component (SAP; Dl-SAP-Mu; Bio-connect, The Netherlands) was analyzed in the plasma isolated from orbital blood using the ELISA protocol. Absorbances were measured at 450 nm and 570 nm.

2.3. Whole blood assay

A whole blood cytokine release assay was performed according to the protocol of De Groote et al. [21]. After sacrifice, orbital blood was collected into EDTA tubes, and directly diluted (1:5) in RPMI 1640 medium containing 1% penicillin and 1% L-glutamine without fetal bovine serum and incubated with 1 ng/ml lipopolysaccharide (LPS) for 6 h at 37 °C to stimulate TNFα production by monocytes. Subsequently, supernatant was collected after 5-min centrifugation at 1500 rpm. Tnfα concentration in the supernatant was measured using an ELISA assay (BD bioscience, USA). Absorbances were measured at 450 nm and 570 nm.

2.4. Plasma insulin and blood glucose measurements

Blood glucose levels were measured using a Bayer Contour TS glucose meter (Leverkusen, Germany). Plasma was collected after 5-min centrifugation at 5000 rpm of the orbital blood to determine insulin concentrations by ELISA (Alpco, Salem, NH, USA).

2.5. Plasma lipid measurements

Plasma specimens were isolated from orbital blood samples after 5-min centrifugation at 5000 rpm. Concentrations of total cholesterol and triglycerides in plasma specimens were determined using enzymatic colorimetric assays (Roche Diagnostics).

2.6. Gene expression analysis

Total RNA was isolated from snap-frozen organs according to the standard protocol of Chomczynski and Sacchi [22]. In short, RNA was converted into cDNA using Maxima H Minus Reverse Transcriptase. After adding the SensiMix SYBR low-ROX mix, the PCR cycle threshold (Ct) values were measured using the ABI 7500 Real Time PCR system (Applied Biosystems, Foster City, CA, USA). As housekeeping genes, the average Ct values of acidic ribosomal phosphoprotein P0 (*36b4*), hypoxanthine guanine phosphoribosyl transferase (*Hprt*), and ribosomal protein L27 (*Rpl27*) were used. Primer sequences of the housekeeping genes and the genes of interest can be found in Table 1.

2.7. Histological analysis

Hearts were formalin fixed (3.7% neutral-buffer formalin; Shandon Formal-Fixx, Thermo scientific, Runcorn, UK) and embedded in OCT compound (Optimum Cutting Temperature; Sakura Finetek Europe B·V., Alphen aan de Rijn, The Netherlands) before sectioning. Cryosections of 10 μm were collected in Menzel Gläser SuperFrost® Plus slides (Thermo Scientific; USA). Plaque size per valve was determined after staining of cryosections for neutral lipids using Oil Red O and hematoxylin (Sigma-Aldrich, Zwijndrecht, The Netherlands). For the macrophage staining, a primary monoclonal rat-*anti*-mouse Cd68 antibody (FA-11; ab53444; Abcam, Cambridge, UK) was used after 1:1000 dilution in blocking

Table 1
Nucleotide sequences of primers used for RT-PCR.

Gene	GenBank Accession no.	Forward primer	Reverse primer
Hprt	NM_013556.2	GCTGGTGAAAAGGACCTCTCGAAGT	CAACTTGCGCTCATCTTAGGCTTTGT
Rpl27	NM_011289.3	CGCCAAGCGATCCAAGATCAAGTCC	AGCTGGGTCCCTGAACACATCCTTG
36b4	NM_007475.5	CTGAGTACACCTTCCCACTTACTGA	CGACTCTTCCTTTGCTTCAGCTTT
Atgl/Pnpla2	NM_001163689.1	GCCAACGCCACTCACATCTACGG	GAGGGATGCAGAGGACCCAGGAAC
Lipe/Hsl	NM_010719.5	GCCTACTGCTGGGCTGTCAAGC	AGGGACACAGTGATGCAGAGATTCCC
Mgll	NM_001166251.1	GGGTTCTGCTGACCGGCTTTGC	CCTGTGGAGGACGTGATAGGCACC
Lpl	NM_008509.2	CCCCTAGACAACGTCCACCTC	TGGGGGCTTCTGCATACTCAAA
Cd36	NM_001159558.1	ATGGTAGAGATGGCCTTACTTGGG	AGATGTAGCCAGTGTATATGTAGGCTC
Ins1	NM_008386.4	CCCCAGCCCTTAGTGACCAGCTATA	AGATGCTGTTTGACAAAAGCCTGGGT
Ins2	NM_001185083.2	ACCAGCCCTAAGTGATCCGCTACAA	ACACACCAGGTAGAGAGCCTCCAC
G6pc	NM_008061.4	CCAGGTCGTGGCTGGAGTCTTG	GCGCGAAACCAAACAAGAAGATGGT
Gys1	NM_030678.3	CTTCCCCTCCTACTATGAGCCCTGG	TGTGAGCATGAATCATCCAGGCTGC
Pygm	NM_011224.2	GAGAACTTCTTCATCTTCGGCATGCG	TGTTCGATGATCTGCCGAAGCTCAG
Gck	NM_010292.5	CGTGGTGCTTTTGAGACCCGTTTTG	GAGTGCTCAGGATGTTAAGGATCTGCC
Fasn	NM_007988.3	GGCGGCACCTATGGCGAGG	CTCCAGCAGTGTGCGGTGGTC

buffer. A secondary AP-conjugated goat-*anti*-rat IgG (A8438, Sigma-Aldrich, Zwijndrecht, The Netherlands) was used at a dilution of 1:100 in blocking buffer. The ready-to use BCIP®/NBT liquid substrate system (sigma-Aldrich, Zwijndrecht, The Netherlands) was used for detection. Corresponding sections were stained using the Masson's Trichrome method (Sigma-Aldrich) to determine collagen content. Mean lesion, macrophage, and collagen area (μm [2]) were quantified using pictures generated with a digital slide scanner (PANNORAMIC 250 Flash II, 3dHistech) and image J software. Quantification was performed blinded.

2.8. Statistical analysis

All statistical tests were performed using the GraphPad Prism 8.0 Software (2020). Outliers were detected using a Grubb's test. Depending on the number of variables in the data, a one-way ANOVA or two-way ANOVA with Bonferroni post-test was performed. To investigate potential TP-064 dose dependency, one-way ANOVA trend tests were performed. Correlation analysis was performed with the linear regression test. All data in bar graphs are presented as means with SEM. Significance between treatment groups and the control group is indicated with * ($p < 0.05$), ** ($p < 0.01$) or *** ($p < 0.001$). Significant dose-dependent trends within all groups are presented in the graphs by an arrow with $^{\#}$ ($p < 0.05$), $^{\#\#}$($p < 0.01$) and $^{\#\#\#}$($p < 0.001$).

3. Results

3.1. TP-064 treatment lowers LPS-induced TNFα secretion by blood monocytes in a dose-dependent manner ex vivo

In order to investigate the effects of PRMT4 inhibition in atherosclerosis-prone mice, male *apoe*$^{-/-}$ mice fed a Western-type diet

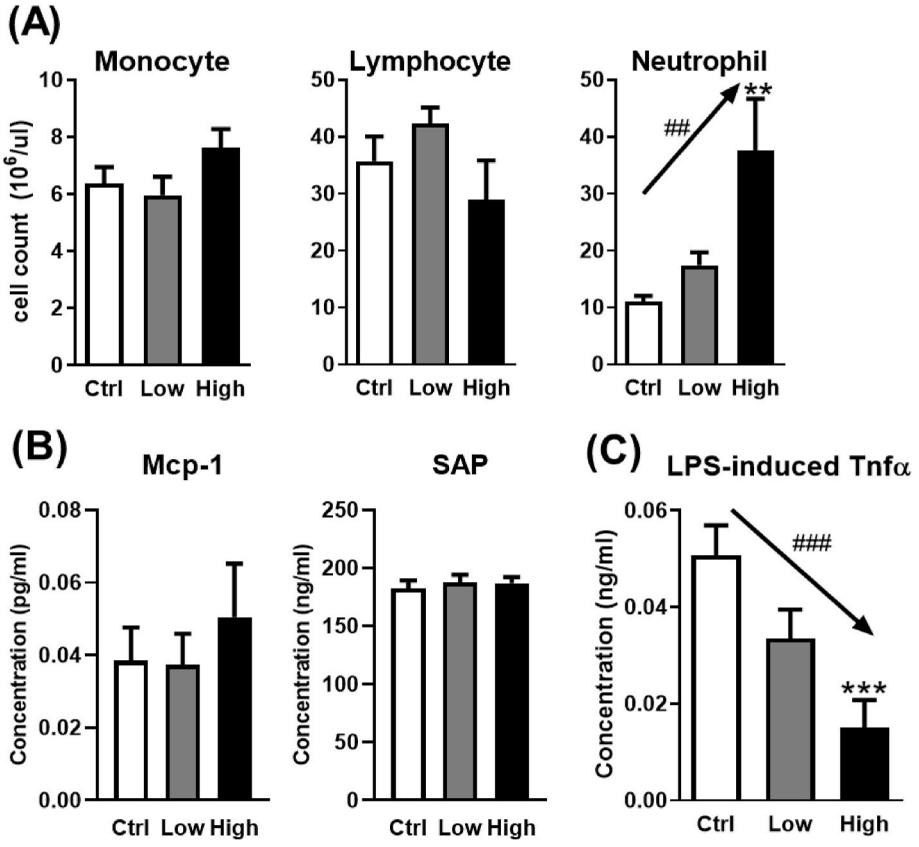

Fig. 1. TP-064 treatment lowers LPS-induced Tnfα secretion by blood monocyte in a dose-dependent manner *ex vivo*.
(A) Blood monocyte, lymphocyte, and neutrophil counts in the orbital blood samples collected from *apoe*$^{-/-}$ mice treated with DMSO solvent control (Ctrl) or 2.5 mg/kg (Low) or 10 mg/kg (High) TP-064. (B) Concentration of pro-inflammatory mediators Mcp-1 and SAP in plasma samples from different groups of mice. (C) Tnfα production in cultured orbital blood samples after 6-h LPS (1 ng/ml) exposure. Data are expressed as means ± SEM. $^{**}p < 0.01$, $^{***}p < 0.001$ (one-way ANOVA), $^{\#\#}p < 0.01$, $^{\#\#\#}p < 0.001$ (one-way ANOVA trend test).

were given 3 times per week an intraperitoneal injection with either 2.5 mg/kg bodyweight (low dose) or 10 mg/kg bodyweight (high dose) TP-064 or the solvent control DMSO for a period of 6 weeks. After sacrifice, the number of blood leukocytes was measured directly, which showed that the cell counts of monocytes and lymphocytes were not changed by TP-064 treatment. In line with our previous finding that TP-064 at a dosage of 10 mg/kg bodyweight promotes neutrophilia in wild-type mice due to its nuclear factor kappa-light-chain-enhancer of activated B cells (NF-kB) inhibitory action [8], we observed that TP-064 induced a significant increase of neutrophil numbers in high dose-treated mice (one-way ANOVA: $p < 0.01$). The increase in blood neutrophil counts was not significant in low dose-treated mice (Fig. 1A). The TP-064-induced neutrophilia did not translate into any changes in plasma concentrations of the pro-inflammatory mediators monocyte chemoattractant protein-1 (Mcp-1) and serum amyloid P component (SAP) (Fig. 1B). However, an *ex vivo* whole blood assay showed that TP-064 treatment dose-dependently decreased the LPS-induced NF-kB-induced Tnfα secretion by blood monocytes (one-way ANOVA: $p < 0.001$ for trend). As shown in Fig. 1C, Tnfα secretion by blood cells from low dose TP-064-treated mice was 30% ($p = 0.097$) lower and 70% ($p < 0.001$) by cells from high dose TP-064-treated mice.

3.2. TP-064 treatment dose-dependently lowers expression levels of PPARγ target genes in white adipose tissue and is associated with reduced bodyweight gain

After 6 weeks of Western-type diet feeding, we found that mice from the high dose TP-064 treatment group had not gained weight, while mice from the control and low dose groups had gained around 1.4 g ($p < 0.001$; Fig. 2A). Bodyweight gain in mice under Western-type diet feeding conditions is driven by adipogenesis [23]. In line with the previous *in vitro* study by Yadav et al., which suggested that PRMT4 plays an essential role in lipid metabolism of adipose tissue via PPARγ signaling [13], we consistently found that the PPARγ target genes lipoprotein lipase (*Lpl*) and fatty acid translocase (*Cd36*) were dose-dependently downregulated by TP-064 treatment (one-way ANOVA trend test: $p < 0.001$; Fig. 2B). In accordance with the study of Li et al. [24], we also showed that TP-064 significantly downregulated the mRNA expression of the three PRMT4-PPARγ-regulated lipolysis genes adipose triglyceride lipase (*Atgl/Pnpla2*), hormone-sensitive lipase (*Hsl/Lipe*), and monoacylglycerol lipase (*Mgll*) in a dose-dependent manner (one-way ANOVA trend test: $p < 0.001$; Fig. 2B). Importantly, in line with the assumption that the dose-dependent effect of PRMT4 inhibition by TP-064 on adipocyte gene expression underlies the effect on body weight gain, we detected a very significant correlation between *Lpl* gene expression levels and body weight gain in the individual mice (correlation coefficient $r = 0.69$; $p < 0.001$; Fig. 2C).

3.3. TP-064 treatment dose-dependently downregulates glycogen metabolism-related gene expression in liver but not in muscle

Herzig et al. showed that PRMT4 is required for the activation of the glycogenolysis gene *G6pc* in hepatocytes *in vitro* [15]. In accordance, TP-064-mediated inhibition of PRMT4 activity was associated with a dose-dependent decrease in hepatic *G6pc* mRNA expression levels (one-way ANOVA trend test: $p < 0.001$). More specifically, on average 52 ± 14% lower *G6pc* gene expression levels were detected in livers of low dose-treated mice ($p < 0.05$) and 75 ± 6% lower levels in high dose-treated mice ($p < 0.001$) as compared to controls (Fig. 3A). Wang et al. have shown, *in vitro*, that PRMT4 modulates the expression levels of *Gys1* and *Pygm* genes involved in skeletal muscle glycogen metabolism [16]. However, our current *in vivo* study showed that *Gys1* and *Pygm* expression levels in calf muscle were not affected by TP-064-mediated PRMT4 inhibition ($p > 0.05$; Fig. 3B).

3.4. TP-064 treatment tends to reduce plasma insulin levels and downregulates mRNA expression levels of insulin target genes in the liver

Kim et al. have shown that PRMT4 is involved in insulin secretion by pancreatic beta cells *in vitro* [14]. We accordingly found that the mRNA

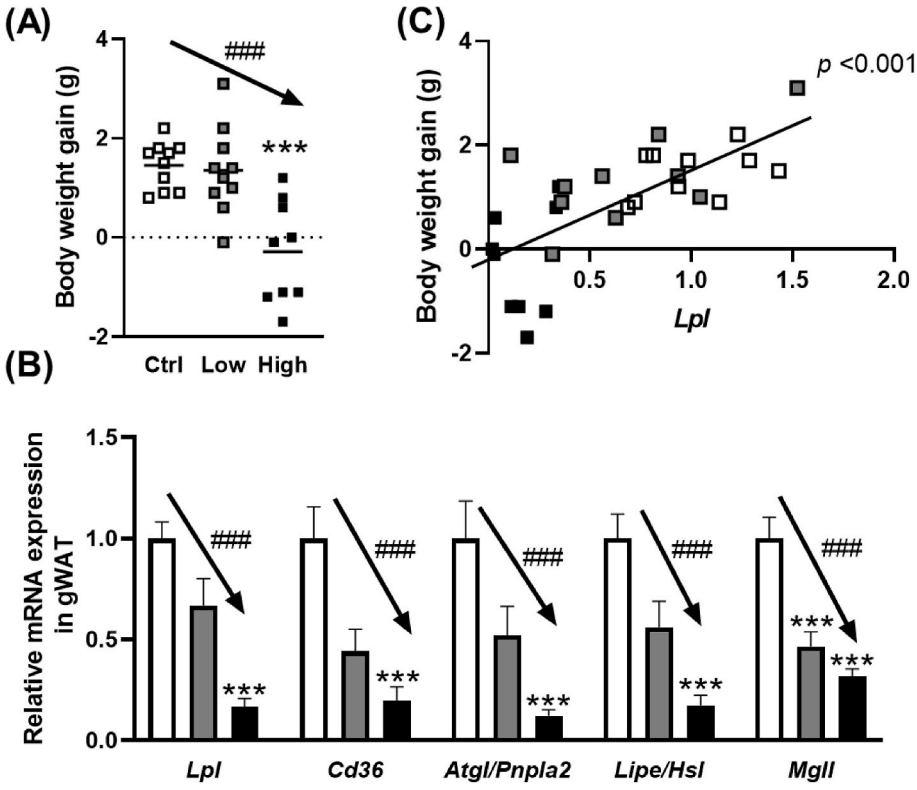

Fig. 2. TP-064 treatment dose-dependently lowers expression levels of PPARγ target genes in white adipose tissue and is associated with reduced bodyweight gain.
(A) Body weight gain from *apoe*$^{-/-}$ mice treated with DMSO solvent (Ctrl; white) or 2.5 mg/kg (Low; grey) or 10 mg/kg (High; black) TP-064 for 8 weeks under Western-type diet feeding conditions. (B) Relative mRNA expression levels of PPARγ target genes in gonadal white adipose tissue. (C) Plasma triglyceride and total cholesterol levels in the different groups of mice. Data are expressed as means ± SEM. $^{***}p < 0.001$ (one-way ANOVA), $^{###}p < 0.001$ (one-way ANOVA trend test).

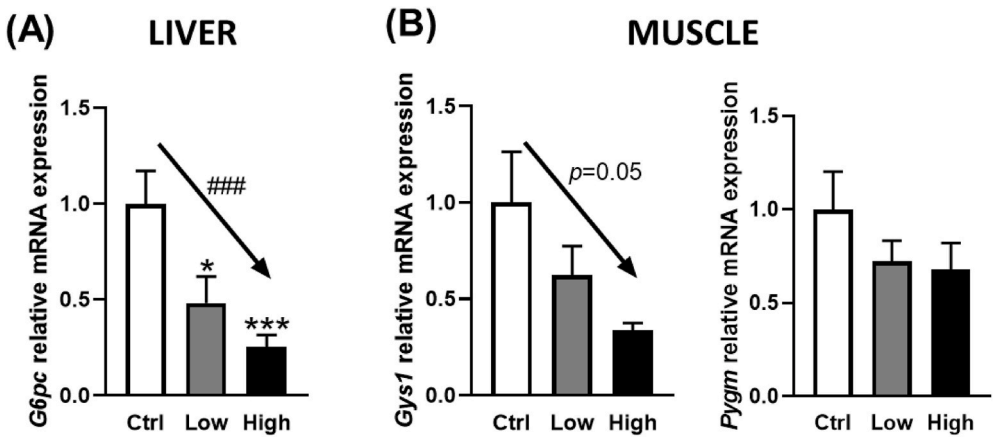

Fig. 3. TP-064 treatment dose-dependently downregulates glycogen metabolism related gene expression in the liver but not in the muscle.
Relative mRNA expression levels of the glycogen metabolism-related genes *G6pc* in the liver (A) and *Gys1* and *Pygm* in calf muscle (B). Data are expressed as means ± SEM. $^{*}p < 0.05$, $^{***}p < 0.001$ (one-way ANOVA), $^{\#\#\#}p < 0.001$ (one-way ANOVA trend test).

expression levels of both insulin 1 (*Ins1*) and 2 (*Ins2*) were somewhat reduced in high dose TP-064-treated mice as compared to the control group (two-way ANOVA: $p < 0.05$ for treatment; Fig. 4A). In accordance, we observed that plasma insulin concentrations in TP-064-treated mice tended to be lower as compared to control mice (one-way ANOVA trend test: $p = 0.10$). Probably as a result, non-fasting plasma glucose levels were higher in TP-064-treated mice as compared to controls (one-way ANOVA trend test: $p = 0.07$; Fig. 4B). In addition, significant downregulation of the mRNA expression levels of insulin target genes *Gck* (−47%; $p < 0.001$) and *Fasn* (−54%; $p < 0.001$) was found in high dose-treated livers (Fig. 4C). *Fasn* is a key regulator of hepatic triglyceride synthesis and secretion [25]. In line with the lower hepatic *Fasn* expression levels, a significantly lower plasma triglyceride concentration was found in high dose TP-064-treated mice (−30%; $p < 0.05$). However, plasma cholesterol levels were similar in all groups of mice (Fig. 4D).

3.5. TP-064 treatment does not significantly change atherosclerosis susceptibility

To measure the effect of TP-06 treatment on atherosclerosis burden, sections from the aortic root were stained with Oil Red O to identify neutral lipids, with *anti*-Cd68 to stain macrophages and Masson's Trichrome to detect collagen (Fig. 5A). Oil Red O lipid staining showed average atherosclerotic lesion areas of 94×10^3 μm [2] in control mice (Fig. 5B). Quantification of macrophage and collagen areas showed that almost 80%–90% of the plaques was composed of macrophages (Fig. 5C and D) and only around 1.5% of collagen (Fig. 5E), suggesting that the lesions were in an early stage. Both low and high dose TP-064 treatment did not show any difference in the measured plaque parameters as

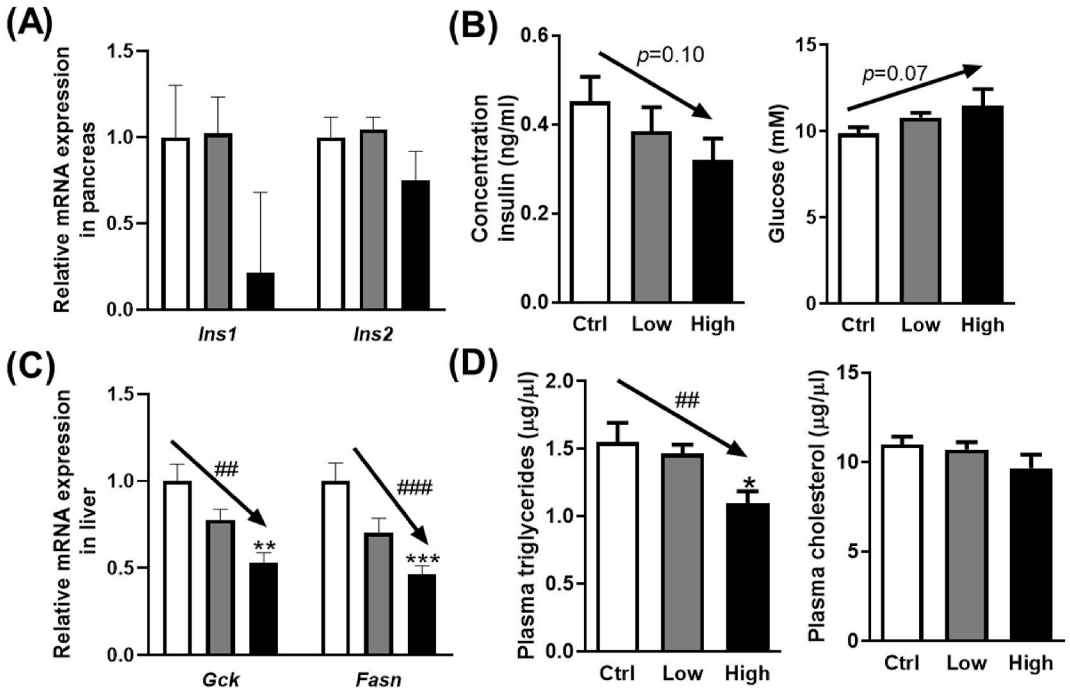

Fig. 4. TP-064 treatment reduces plasma insulin levels and downregulates the mRNA expression levels of insulin target genes in the liver.
Relative mRNA expression levels of (A) insulin genes *Ins1* and *Ins2* in the pancreas and (C) insulin target genes *Gck* and *Fasn* in the liver. (B) Plasma insulin and blood glucose levels in mice treated with DMSO solvent (Ctrl; white), 2.5 mg/kg (Low; grey) or 10 mg/kg (High; black) TP-064. (D) Plasma triglyceride and total cholesterol levels in the different groups of mice. Data are expressed as means ± SEM. $^{***}p < 0.001$ (one-way ANOVA), $^{\#\#}p < 0.01$, $^{\#\#\#}p < 0.001$ (one-way ANOVA trend test).

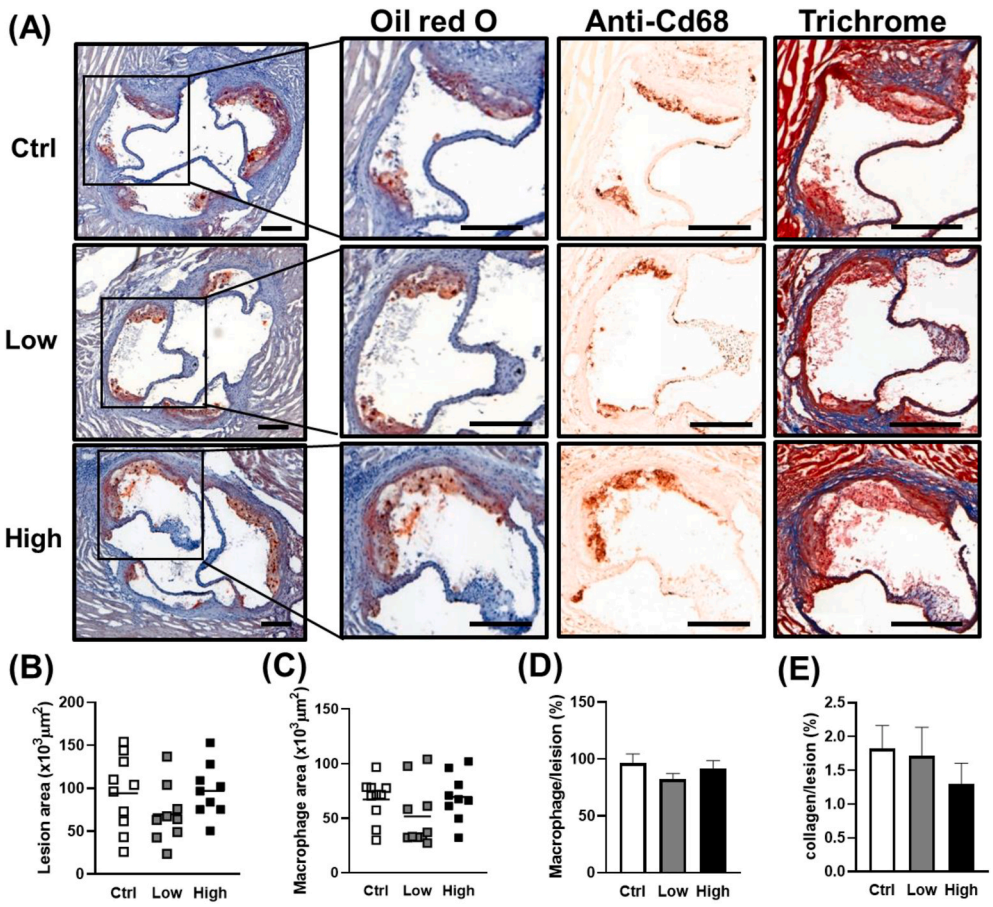

Fig. 5. TP-064 treatment does not significantly change atherosclerosis susceptibility. (A) Representative pictures of aortic root sections stained with Oil Red O (neutral lipids), anti-Cd68 (macrophages) or Masson's Trichrome (collagen). Scale bar = 200 µm. Quantification of the total lesion area (B) and lesional macrophage (C and D) and collagen (E) areas. Data are shown as individual points with the group average as horizontal lines (B and C) or expressed as means ± SEM (D and E). (For interpretation of the references to color in this figure legend, the reader is referred to the Web version of this article.)

compared to control-treated mice (Fig. 5B–E), suggesting a null effect of PRMT4 inhibition on atherosclerosis susceptibility.

4. Discussion

Using the PRMT4 inhibitor TP-064, in the current study, we have highlighted the relevance of PRMT4 function *in vivo*. More specifically, our study showed that TP-064 treatment decreases LPS-activated Tnfα secretion by blood monocytes, even in the context of higher neutrophil counts. In addition, we observed that *in vivo* treatment of TP-064 is able to systemically downregulate PRMT4-dependent signaling pathways, including PPARγ-regulated lipolysis in white adipose tissue, hepatic glycogen metabolism, and insulin levels and signaling. However, TP-064 treatment did not significantly affect atherosclerotic development in male *apoe*$^{-/-}$ mice.

Our finding that *in vivo* TP-064 treatment (1) reduced pro-inflammatory blood monocyte TNFα secretion upon *ex vivo* LPS-stimulation and (2) induced neutrophilia is in line with previous observations that PRMT4 acts as a co-activator of the transcription factor NF-kB [7,8,26]. The inhibition of PRMT4-NF-kB activation by TP-064 did not lower the susceptibility of *apoe*$^{-/-}$ mice for atherosclerotic lesion development. This is in contrast to the study of Liu et al. which showed that drug-induced direct inhibition of NF-kB in pro-inflammatory monocytes/macrophages significantly reduced the severity of aortic atherosclerotic lesions in the same atherosclerotic mouse model [27]. In line with a more complex role of PRMT4 in atherosclerosis, TP-064 treatment also generated other systemic effects, which are considered pro-atherogenic. For example, in agreement with our observation that insulin signaling was blocked by TP-064 treatment in a dose-dependent manner, the studies of Christian et al. [28] and Gonzalez et al. [29] have suggested that hyperglycemia as a result of loss of insulin signaling aggravates lesion development in atherosclerotic mice.

Interestingly, we found that TP-064 treatment *in vivo* significantly affected the expression levels of adipogenic PPARγ target genes. Consistently, Yadav et al. have shown that PRMT4 knockout embryos accumulate less lipid in their brown adipose tissue compared with wild-type embryos. Also, knockdown of PRMT4 in mouse embryonic fibroblasts (3T3-L1 cells) lowered their adipogenic potential due to an impaired conversion into mature adipocytes [13]. In further support, Amit et al. showed an enhanced adipocyte differentiation in PRMT4 overexpressing 3T3-L1 cells [30]. Considering that deletion of *PPARγ* in adipose tissue of mice protects against high fat diet-induced obesity and insulin resistance [31], we hypothesize that TP-064-induced PRMT4 inhibition can be a future therapeutic strategy to target PPARγ-dependent adipogenesis and obesity. In this context, it is important to note that a clinical study by Panach et al. also identified *PRMT4* as a gene highly correlated with obesity and fasting insulin levels in humans. More specifically, they observed a significant association between a PRMT4 single nucleotide polymorphism and body weight, plasma triglyceride and glucose levels [32].

In conclusion, we have shown that TP-064-induced systemic PRMT4 inhibition is associated with both anti-inflammatory and adverse metabolic effects, resulting in an overall null effect on the initiation and formation of early stage lesions in male mice. Our study highlights that PRMT4 plays a physiological role in many different tissues in mice and could be a potential therapeutic target in obesity. Notably, female mice are more susceptible to atherosclerosis and PRMT4 has been shown to act as a coactivator for the nuclear receptor of the female hormone estrogen in breast cancer [33]. It will therefore be interesting to follow up our current findings by studying the effect of TP-064 treatment on metabolism and atherosclerosis also in female mice.

Financial support

This study was supported by grants from the Netherlands Organization for Scientific Research (VICI 91813603) awarded to Miranda Van Eck. Miranda van Eck is head of the Cardiovascular and Metabolic Therapeutics group (https://www.universiteitleiden.nl/en/science/drug-research/biotherapeutics/cardiovascular-and-metabolic-therapeutics) and an Established Investigator of the Dutch Heart Foundation (2007T056). Yiheng Zhang is supported by the Chinese Scholarship Council (CSC).

Declaration of competing interest

The authors declare that they have no known competing financial interests or personal relationships that could have appeared to influence the work reported in this paper.

Acknowledgments

The authors thank Sahel Taei and Mireia N.A. Bernabé Kleijn for excellent technical assistance.

References

[1] M. Peled, E.A. Fisher, Dynamic aspects of macrophage polarization during atherosclerosis progression and regression, Front. Immunol. 5 (2014) 579.
[2] M.T. Bedford, S.G. Clarke, Protein arginine methylation in mammals: who, what, and why, Mol. Cell 33 (2009) 1–13.
[3] J. Fuhrmann, K.W. Clancy, P.R. Thompson, Chemical biology of protein arginine modifications in epigenetic regulation, Chem. Rev. 115 (2015) 5413–5461.
[4] M.T. Bedford, S. Richard, Arginine methylation: an emerging regulatorof protein function, Mol. Cell 18 (2005) 263–272.
[5] F. Bachand, Protein arginine methyltransferases: from unicellular eukaryotes to humans, Eukaryot. Cell 6 (2007) 889–898.
[6] X. Liu, et al., Coactivator-associated arginine methyltransferase 1 targeted by miR-15a regulates inflammation in acute coronary syndrome, Atherosclerosis 233 (2014) 349–356.
[7] M. Covic, et al., Arginine methyltransferase CARM1 is a promoter-specific regulator of NF-κB-dependent gene expression, EMBO J. 24 (2005) 85–96.
[8] Y. Zhang, M. de Boer, E.J. van der Wel, M. Van Eck, M. Hoekstra, PRMT4 inhibitor TP-064 inhibits the pro-inflammatory macrophage lipopolysaccharide response in vitro and ex vivo and induces peritonitis-associated neutrophilia *in vivo*, Biochim. Biophys. Acta (BBA) - Mol. Basis Dis. 1867 (2021) 166212.
[9] C. Yeom, et al., Insulin-induced CARM1 upregulation facilitates hepatocyte proliferation, Biochem. Biophys. Res. Commun. 461 (2015) 568–574.
[10] X.-Y. Zhong, et al., CARM1 methylates GAPDH to regulate glucose metabolism and is suppressed in liver cancer, Cell Rep. 24 (2018) 3207–3223.
[11] F.D. Barr, L.J. Krohmer, J.W. Hamilton, L.A. Sheldon, Disruption of histone modification and CARM1 recruitment by arsenic represses transcription at glucocorticoid receptor-regulated promoters, PLoS One 4 (2009), e6766.
[12] J. Kim, et al., Loss of CARM1 results in hypomethylation of thymocyte cyclic AMP-regulated phosphoprotein and deregulated early T cell development, J. Biol. Chem. 279 (2004) 25339–25344.
[13] N. Yadav, et al., CARM1 promotes adipocyte differentiation by coactivating PPARγ, EMBO Rep. 9 (2008) 193–198.
[14] J.K. Kim, et al., PRMT4 is involved in insulin secretion via the methylation of histone H3 in pancreatic β cells, J. Mol. Endocrinol. 54 (2015) 315–324.
[15] A. Krones-Herzig, et al., Signal-dependent control of gluconeogenic key enzyme genes through coactivator-associated arginine methyltransferase 1, J. Biol. Chem. 281 (2006) 3025–3029.
[16] S.-C.M. Wang, D.H. Dowhan, N.A. Eriksson, G.E.O. Muscat, CARM1/PRMT4 is necessary for the glycogen gene expression programme in skeletal muscle cells, Biochem. J. 444 (2012) 323–331.
[17] N. Yadav, et al., Specific protein methylation defects and gene expression perturbations in coactivator-associated arginine methyltransferase 1-deficient mice, Proc. Natl. Acad. Sci. Unit. States Am. 100 (2003) 6464–6468.
[18] A.E. Drew, et al., Identification of a CARM1 inhibitor with potent in vitro and *in vivo* activity in preclinical models of multiple myeloma, Sci. Rep. 7 (2017) 1–13.
[19] K. Nakayama, et al., TP-064, a potent and selective small molecule inhibitor of PRMT4 for multiple myeloma, Oncotarget 9 (2018) 18480.
[20] R.L. Reddick, S.H. Zhang, N. Maeda, Atherosclerosis in mice lacking apo E. Evaluation of lesional development and progression, Arterioscler. Thromb. a J. Vasc. Biol. 14 (1994) 141–147.
[21] D. De Groote, et al., Novel method for the measurement of cytokine production by a one-stage procedure, J. Immunol. Methods 163 (1993) 259–267.
[22] P. Chomczynski, N. Sacchi, Single-step method of RNA isolation by acid guanidinium thiocyanate-phenol-chloroform extraction, Anal. Biochem. 162 (1987) 156–159.
[23] T. Hayashi, et al., Factor for adipocyte differentiation 158 gene disruption prevents the body weight gain and insulin resistance induced by a high-fat diet, Biol. Pharm. Bull. 34 (2011) 1257–1263.
[24] Y. Li, et al., Protein arginine methyltransferase 4 regulates adipose tissue lipolysis in type 1 diabetic mice, Diabetes, Metab. Syndrome Obes. Targets Ther. 13 (2020) 535.
[25] X. Lin, G. Schonfeld, P. Yue, Z. Chen, Hepatic fatty acid synthesis is suppressed in mice with fatty livers due to targeted apolipoprotein B38. 9 mutation, Arterioscler. Thromb. Vasc. Biol. 22 (2002) 476–482.
[26] F. Miao, S. Li, V. Chavez, L. Lanting, R. Natarajan, Coactivator-associated arginine methyltransferase-1 enhances nuclear factor-κB-mediated gene transcription through methylation of histone H3 at arginine 17, Mol. Endocrinol. 20 (2006) 1562–1573.
[27] S.-L. Liu, et al., A novel inhibitory effect of naloxone on Macrophage Activation and Atherosclerosis Formation in Mice, J. Am. Coll. Cardiol. 48 (2006) 1871–1879.
[28] C. Rask-Madsen, et al., Loss of insulin signaling in vascular endothelial cells accelerates atherosclerosis in apolipoprotein E null mice, Cell Metabol. 11 (2010) 379–389.
[29] L. Gonzalez, M.E. MacDonald, Y.D. Deng, B.L. Trigatti, Hyperglycemia aggravates diet-induced coronary artery disease and myocardial infarction in SR-B1-Knockout/ApoE-Hypomorphic mice, Front. Physiol. 9 (2018) 1398.
[30] A.K. Behera, A. Bhattacharya, M. Vasudevan, T.K. Kundu, p53 mediated regulation of coactivator associated arginine methyltransferase 1 (CARM1) expression is critical for suppression of adipogenesis, FEBS J. 285 (2018) 1730–1744.
[31] J.R. Jones, et al., Deletion of PPARγ in adipose tissues of mice protects against high fat diet-induced obesity and insulin resistance, Proc. Natl. Acad. Sci. Unit. States Am. 102 (2005) 6207–6212.
[32] L. Panach, et al., Comparative transcriptome analysis identifies CARM1 and DNMT3A as genes associated with osteoporosis, Sci. Rep. 10 (2020) 1–10.
[33] B. Peng, et al., A hypermethylation strategy utilized by enhancer-bound CARM1 to promote estrogen receptor α-dependent transcriptional activation and breast carcinogenesis, Theranostics 10 (2020) 3451.